

# Origin of Low Thermal Conductivity in Nuclear Fuels

Quan Yin and Sergey Y. Savrasov

*Department of Physics, University of California, Davis, CA 95616*

(Dated: October 29, 2018)

Using a novel many-body approach, we report lattice dynamical properties of  $\text{UO}_2$  and  $\text{PuO}_2$  and uncover various contributions to their thermal conductivities. Via calculated Grüneisen constants, we show that only longitudinal acoustic modes having large phonon group velocities are efficient heat carriers. Despite the fact that some optical modes also show their velocities which are extremely large, they do not participate in the heat transfer due to their unusual anharmonicity. Ways to improve thermal conductivity in these materials are discussed.

Today's nuclear fuels are based on  $^{235}\text{U}$  and  $^{239}\text{Pu}$  elements where in a typical set-up, a nuclear reaction heats up a pellet made of either  $\text{UO}_2$  or its mixture with  $\text{PuO}_2$  and the heat is transformed to electrical energy. One of the major issues is to conduct the heat from a core of the pellet to its outer area which makes the evaluation of a high temperature thermal conductivity a key problem. Unfortunately, the thermal conductivity of  $\text{UO}_2$  is very low and as a result, even a gradual increase of its value may lead to significant breakthrough in the performance of commercial nuclear reactors currently operating worldwide.

In the present work, we argue that it is the unexpectedly large anharmonicity of optical modes that results in a very low thermal conductivity of modern nuclear fuels. Consider semiconducting  $\text{UO}_2$  which is a main element of UOX fuel, or a blend of U and Pu oxides which is a major substance of MOX fuel. The heat from the core of the pellet in these insulating systems is carried by phonons which are known to be very inefficient heat conductors. This brings a whole set of complex problems such as causing fuel pellets to crack and degrade prematurely, necessitating replacement before the fuel has been depleted.

Unfortunately, studying thermal conductivity [1] as well as such properties as crystal structures, phase diagrams, lattice dynamics and structural instabilities of the actinide based materials is a formidable theoretical problem. Most of the previous works have concentrated on molecular dynamic simulations with empirically adjusted interatomic potentials [2][3]. However, the  $5f$  electrons in actinides are close to a localization-delocalization or Mott transition as it has been recently demonstrated for Plutonium metal [4][5][6].  $\text{UO}_2$  and  $\text{PuO}_2$  are Mott-Hubbard insulators with energy gaps at both low and high temperatures. Despite an impressive set of past theoretical studies [7][8][9][10][11], the spectral functions of the high temperature paramagnetic regime cannot be obtained by static-mean field theories such as the Density Functional Theory [12] and require a genuine many-body treatment.

In the present work we use a novel electronic structure method [13] capable of describing Mott insulating materials in order to address the structural properties and thermal conductivity of the modern nuclear fuels. Both  $\text{UO}_2$

and  $\text{PuO}_2$  are calculated using a combination of local density approximation (LDA) [12] and Dynamical Mean Field Theory (DMFT) [14][15] where relativistic  $5f$  shells of Uranium and Plutonium atoms are treated by exact diagonalization of corresponding many-body Hamiltonians obtained by allowing a hybridization between the  $5f$ -electrons and the nearest oxygen  $2p$  orbitals.

It is well known that a strong spin-orbit coupling of about  $1eV$  present in actinides splits 14-fold degenerate  $f$  level onto  $f_{5/2}$  and  $f_{7/2}$  states. Group theoretical considerations assume that under cubic crystal symmetry, the  $f_{5/2}$  6-fold degenerate level is further split onto  $\Gamma_8$  quadruplet and  $\Gamma_7$  doublet. In both  $\text{UO}_2$  and  $\text{PuO}_2$ , the  $\Gamma_8$  level comes approximately  $0.1eV$  below the  $\Gamma_7$  state, and valence arguments make it occupied by two electrons for the case of  $\text{UO}_2$  and fully occupied by four electrons for the case of  $\text{PuO}_2$ . This sequence of the levels dictates the low temperature properties of these two materials: The  $\text{UO}_2$  becomes magnetic where the 9-fold degenerate many-body ground state of the atomic  $f$ -shell  $^3\text{H}_4$  with  $J = 4$  is split onto 4 subsets, among which the lowest triplet state of  $\Gamma_5$  symmetry carries the moment of about  $1.7 - 1.8\mu_B$  below the Néel temperature of  $30.8K$  [16]. On the other hand,  $\text{PuO}_2$  has the filled  $\Gamma_8$  one-electron level, making its atomic  $^3\text{K}_4$  multiplet split in such way that the non-magnetic  $\Gamma_1$  singlet comes lowest.

The cluster exact diagonalizations which are carried out in our LDA+DMFT calculations support this atomic physics picture and only marginally alter the self-energies for the  $f$ -electrons from their corresponding atomic values. In fact, the crystal structures of both materials show that the actinide elements are centered in the cubic environment (see Fig.1) assuming that only relativistic  $\Gamma_7$  orbital (its shape is shown in Fig.1) of the  $f_{5/2}$  state is properly coordinated by and strongly hybridized with the O  $2p$  states. The corresponding hybridization functions  $\Delta_\alpha(\omega)$  are well fit by the single pole approximation,  $\Delta_\alpha(\omega) = |V_\alpha|^2 / (\omega - P_\alpha)$ , producing only significant values of the matrix elements  $V_\alpha \sim 1eV$  for  $\Gamma_7$  in the  $j = 5/2$  manifold and several times smaller values for the  $\Gamma_8$  orbitals. Similar effect is seen for  $\Gamma_6$ ,  $\Gamma_7$ ,  $\Gamma_8$  states in the  $j = 7/2$  manifold. The position of the dispersive oxygen band centered at the pole  $P_\alpha$  comes out  $-1 \div -5eV$  be-

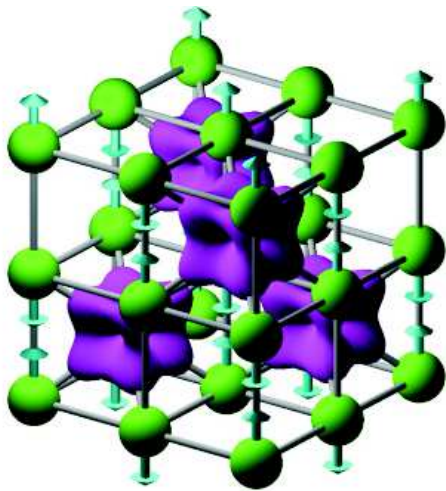


FIG. 1: Crystal structure of  $\text{UO}_2$  and  $\text{PuO}_2$ : Uranium or Plutonium atoms (their shapes are shown by the  $\Gamma_7$  relativistic orbitals) are centered inside the cubic lattice made by oxygen atoms. The arrows show the displacements of oxygens associated with the dispersive longitudinal optical mode.

low the occupied  $f$  states, making both materials classical Mott-Hubbard insulators. We find that the fundamental energy gaps produced by the lower (occupied) and upper (unoccupied) Hubbard bands are equal to  $2.2\text{eV}$  for  $\text{UO}_2$  and  $2.5\text{eV}$  for  $\text{PuO}_2$ . The experimental energy gap in  $\text{UO}_2$  is of the order of  $2\text{eV}$  [16]. These data are obtained utilizing a recently developed matrix expansion algorithm [17] which helps to perform full self-consistency with respect to both the charge densities as required by the LDA procedure and the  $5f$ -electron spectral functions as required by the DMFT. Here, the  $5f$ -electron self-energies extracted from the cluster exact diagonalization are subsequently fit using three-pole interpolation. An effective parameter  $U_{eff} = 3\text{eV}$  describing the on-site Coulomb repulsion among the  $5f$  electrons is used while the other Slater integrals ( $F^{(2)}$ ,  $F^{(4)}$  and  $F^{(6)}$ ) are computed from atomic physics, and are subsequently rescaled to 80% of their values to account for the effect of screening [18].

In order to calculate the phonon spectra of  $\text{UO}_2$  and  $\text{PuO}_2$  we utilize a new relativistic linear response phonon method which has been recently generalized for the LDA+DMFT scheme [19] and has recently demonstrated its predicted power by finding the phonon spectrum of  $\delta$ -Pu metal [20] prior to the experiment [21]. In this linear response calculation the pole interpolation for the self-energies reduces the calculation of the dynamical matrix to standard linear response theory. Since our interest lies in the thermal conductivity at operating temperatures of nuclear fuels, we perform the calculations of the phonon dispersions for paramagnetic phases of the materials with the  $f$ -electron self-energies extracted at  $T = 1000\text{K}$ , where not only the many-body ground states

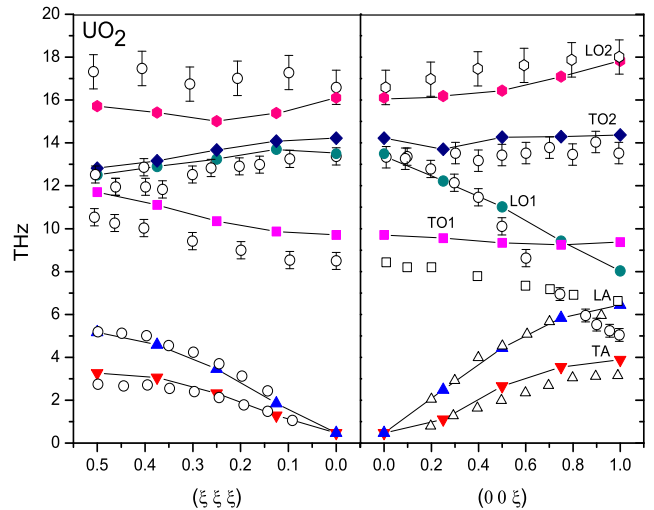


FIG. 2: Calculated phonon dispersions (filled symbols connected by lines) and experimentally measured phonons (open symbols) [16] for  $\text{UO}_2$ .

( $\Gamma_5$  for  $\text{UO}_2$  and  $\Gamma_1$  for  $\text{PuO}_2$ ) but also various low-lying excited states are beginning to contribute.

Fig.2 shows the comparison between our calculated (filled symbols connected by lines) and measured (open symbols) [16] phonon spectrum for  $\text{UO}_2$  along two symmetry lines of the Brillouin Zone. Fig.3 presents our predicted phonon spectrum for  $\text{PuO}_2$ . Overall, both materials demonstrate very similar dispersions. Due to various numerical inaccuracies and approximate treatment of many-body effects, which, in particular, involves the use of  $U_{eff}$ , the overall mismatch between our theory and experiment for  $\text{UO}_2$  is about 15%. The same accuracy can be assumed for our predicted phonon dispersions in  $\text{PuO}_2$ . Increasing the  $U_{eff}$  to 4–5 eV marginally affects the overall phonon spectra although makes all modes somewhat harder.

Our calculations reveal the following features of lattice dynamics in these materials. First, acoustic modes are located at the low frequency region of the spectrum producing the group velocities of about  $700\text{m/s}$  for transverse acoustic (TA) and  $1100\text{m/s}$  for longitudinal acoustic (LA) modes (see also Table 1). There are two groups of transverse and longitudinal optical modes which we schematically label as TO1, LO1 and TO2, LO2. The first group represents lattice vibrations associated with the out-of-phase displacements of oxygens and little involvement of U or Pu atoms. The second group represents the lattice vibrations of oxygens which vibrate in-phase against U or Pu atoms.

There is a remarkably dispersive mode LO1 which has a very large group velocity along (001) direction in both materials. This mode is primarily oxygen based and at the BZ center it is described by polarization vectors as

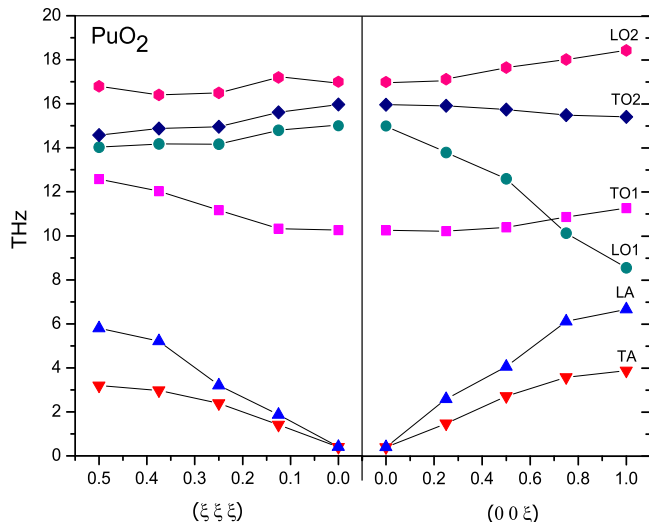


FIG. 3: Calculated phonon dispersions (filled symbols connected by lines) for  $\text{PuO}_2$ . No experiment available.

shown on Fig.1. We see that our theory correctly predicts a softening of this mode as it approaches the zone boundary  $X$  point although it underestimates the experimental value of the frequency by a factor of two for  $\text{UO}_2$  and, most likely, also for  $\text{PuO}_2$ . Note that similar discrepancies have been detected by us earlier in studying lattice vibrations of Plutonium metal [20][21].

As we have gained access to the phonon dispersions, we are ready to discuss the lattice thermal conductivity in these systems which can be expressed for a cubic solid via the phonon frequencies  $\omega_{\mathbf{q}j}$ , group velocities  $v_{\mathbf{q}j}$ , phonon mean free paths  $l_{\mathbf{q}j}$  and the Bose–Einstein distribution functions  $N_{\mathbf{q}j}$  as follows [1]:

$$\kappa = \sum_{\mathbf{q},j} \omega_{\mathbf{q}j} v_{\mathbf{q}j} l_{\mathbf{q}j} \frac{\partial N_{\mathbf{q}j}}{\partial T} \quad (1)$$

It is generally known that various scattering processes determine the temperature dependent phonon mean free paths. These, for example, include normal phonon-phonon interactions where one phonon with wave vector  $\mathbf{q}$  gets scattered with the creation of two phonons with wave vectors  $\mathbf{q}_1$  and  $\mathbf{q}_2$  such that  $\mathbf{q} = \mathbf{q}_1 + \mathbf{q}_2$ , and Umklapp phonon scattering processes where the quasi-momentum conservation involves reciprocal lattice vector  $\mathbf{G}$  such that  $\mathbf{q} = \mathbf{q}_1 + \mathbf{q}_2 + \mathbf{G}$ . At high temperatures which we are interested in the present work, only Umklapp processes are significant [1], and the phonon mean free paths can be evaluated from the knowledge of the third-order anharmonicity coefficients, which can be approximated by the dimensionless Grüneisen constants describing the change in the phonon frequency with respect to the atomic volume, i.e.  $\gamma_{\mathbf{q}j} = d \ln \omega_{\mathbf{q}j} / d \ln V$ . Hence, the efficiency of each phonon mode in the heat conduc-

tion is directly related to its group velocity but reversely proportional to the square of its Grüneisen constant [1].

Looking at the phonon spectra presented in Fig.2 and Fig.3, it is now clear that the best heat carriers are either the acoustic branches or the longitudinal optical branch LO1 which, in fact, has anomalously large group velocity along (001) (experimentally, its  $v_{\mathbf{q}j}$  is twice the LA branch!). One may then pose a question that why  $\text{UO}_2$  or  $\text{PuO}_2$  are known to be such inefficient thermal conductors. When compared to most semiconducting solids where optical modes exhibit rather weak wave vector dispersions and thus do not participate in the heat transfer, here the situation is much more favorable. The answer lies in the anomalously large anharmonicity associated with the LO1 mode, making its mean free path significantly shorter.

To make a comparative analysis, we have calculated the Grüneisen constants  $\gamma_{\mathbf{q}j}$  associated with each vibrational mode at the  $\Gamma$  and  $X$  points of the Brillouin Zone. The results of these calculations are summarized in Table 1. As one can see the transverse acoustic modes have relatively large anharmonicity characterized by  $\gamma = -1.41$  and  $\gamma = -1.59$  for  $\text{UO}_2$  and  $\text{PuO}_2$  respectively. These values remarkably decrease for the LA modes ( $\gamma = -0.50$  and  $-0.54$ ) which at the same time show large group velocity. However, they become huge for the most dispersive LO1 mode. Here, the frequency at  $\Gamma$  shows positive  $\gamma$  (equal to 0.43 and 0.27) meaning that it decreases upon compression while the frequency at  $X$  shows negative  $\gamma$  (equal to  $-2.17$  and  $-2.49$ ) meaning its increase upon compression. Effectively, these two effects will add up to each other and result in the effective Grüneisen constants equal to  $-2.60$  for  $\text{UO}_2$  and  $-2.76$  for  $\text{PuO}_2$ .

With these data in hands we are able to estimate contributions to the lattice thermal conductivity  $\kappa$  from various phonon modes. Using a simple Debye-like linear approximation for the phonon dispersion and including corrections found empirically for the optical branches [22], the results of such estimates at a temperature  $T = 1000\text{K}$  are presented in the last column of Table 1. We can conclude that the only efficient heat carriers in both nuclear materials are their longitudinal acoustic phonons. The TA modes have relatively small contribution because of their smaller group velocities and relatively large  $\gamma$ , while the LO1 modes also do not contribute due to its huge Grüneisen constants which completely compensate the effect of its largest  $v_{\mathbf{q}j}$ . The other modes have a negligible influence on  $\kappa$ .

The total value of  $\kappa$  in our calculation is a factor of two lower than the experimentally known thermal conductivity of  $\text{UO}_2$  equal to  $3.9\text{Wm}^{-1}\text{K}^{-1}$  at  $T = 1000\text{K}$  [23]. This is naturally connected to the approximate character of treating anharmonic effects. However, we believe that the relative contributions from various branches are captured correctly in our estimates, which gives a fundamentally new insight into the processes and factors that

TABLE I: Calculated phonon frequencies (in THz) and Grüneisen constants at  $\Gamma$  and  $X$  points of the Brillouin zone, the phonon group velocities ( $\times 10^2 m/s$ ) estimated along (001) direction as well as contributions to lattice thermal conductivity ( $Wm^{-1}K^{-1}$ ) at  $T = 1000K$  for  $UO_2$  and  $PuO_2$ .

UO <sub>2</sub>						
Branch	$\omega(\Gamma)$	$\gamma(\Gamma)$	$\omega(X)$	$\gamma(X)$	$v_g$	$\kappa$
TA	0.00	0.00	3.88	-1.41	6.76	0.08
LA	0.00	0.00	6.45	-0.50	11.23	1.68
TO1	9.70	-1.32	9.38	-0.15	-0.55	$\sim 0$
LO1	13.51	0.43	8.03	-2.17	-9.53	0.11
TO2	14.22	-0.20	14.42	-0.62	0.31	$\sim 0$
LO2	16.14	0.62	17.81	-0.45	2.95	$\sim 0$
PuO <sub>2</sub>						
Branch	$\omega(\Gamma)$	$\gamma(\Gamma)$	$\omega(X)$	$\gamma(X)$	$v_g$	$\kappa$
TA	0.00	0.00	3.89	-1.59	6.67	0.08
LA	0.00	0.00	6.68	-0.54	11.48	1.50
TO1	10.21	-1.75	11.27	-0.43	1.84	$\sim 0$
LO1	15.03	0.27	8.56	-2.49	-11.10	0.16
TO2	16.07	-0.52	15.42	-0.95	-1.02	$\sim 0$
LO2	17.15	0.54	18.43	-0.60	2.46	$\sim 0$

control thermal conductivity in these materials. As a result, we finally discuss the origins of the large anharmonicity of the most intriguing longitudinal optical mode LO1. As shown on Fig.1, this mode is primarily oxygen driven. Oxygens are arranged in a cubic lattice with Uranium or Plutonium atoms occupying every other center of the cube. It is then clear that the structure is far from close packing and the displacements of oxygens would involve large third order anharmonic effects. To fix this problem, one may think of mixing these materials with elements filling in the cubic interstitials of the lattice and preventing large ionic excursions. One example could be oxygen overdoped materials  $UO_{2+x}$  and  $PuO_{2+x}$  where the latter one has been recently studied theoretically [7].

To summarize, using the LDA+DMFT method and linear response theory, we have studied lattice dynamical properties of  $UO_2$  and  $PuO_2$ . Contributions to lattice thermal conductivity from various phonon modes were uncovered using the calculated group velocities and the Grüneisen constants. It was found that the dispersive longitudinal optical modes do not participate in the heat transfer due to their large anharmonicity. Material design of systems with the last effect suppressed would open new possibilities to build more efficient fuels for modern

nuclear industries.

The authors are indebted to M. J. Gillan, G. Kotliar, and J. Thompson for useful conversations. The work was supported by the NSF grants No. 0608283, 0606498 and by the US DOE grant No. DE-FG52-06NA2621.

- [1] For a review, see, e.g., *Thermal Conductivity: Theory, Properties, and Applications*, edited by Terry M. Tritt, Kluwer Academic, New York (2004).
- [2] P. J. D. Lindan and M. J. Gillan, J. Phys.: Condens. Matter **3**, 3929 ((1991).
- [3] S. Motoyama, Y. Ichikawa and Y. Hiwatari, A. Oe, Phys. Rev. B **60**, 292 (1999).
- [4] S. Y. Savrasov, G. Kotliar, and E. Abrahams, Nature **410**, 793 (2001).
- [5] G. Lander, Science **301**, 1057 (2003).
- [6] J. H. Shim, K. Haule, G. Kotliar, Nature **446**, 513 (2007).
- [7] L. Petit, A. Svane, Z. Szotek, W. M. Temmerman, Science **301**, 498 (2003).
- [8] X. Wu, A. K. Ray, Eur. Phys. J. B **19**, 345 (2001).
- [9] I. D. Prodan, G. E. Scuseria, J. A. Sordo, K. Kudin, R. Martin, J. Chem. Phys. **123**, 014703 (2005).
- [10] K. Kudin, G. Scuseria, R. Martin, Phys. Rev. Lett. **89**, 266402 (2002).
- [11] M. Colarieti-Tosti, O. Eriksson, L. Nordstrom, J. Wills, and M. S. S. Brooks, Phys. Rev. B **65**, 195102 (2002).
- [12] For a review, see, e.g., *Theory of Inhomogeneous Electron Gas*, edited by S. Lundqvist and S. H. March (Plenum, New York, 1983).
- [13] G. Kotliar, S. Y. Savrasov, K. Haule, V. Oudovenko, O. Parcollet, and C. Marianetti, Rev. Mod. Phys. **78**, 865 (2006).
- [14] A. Georges, G. Kotliar, W. Krauth and M. J. Rozenberg, Rev. Mod. Phys. **68**, 13 (1996).
- [15] G. Kotliar and D. Vollhardt, Physics Today **57**, 53 (2004).
- [16] For a review, see, e.g., J. Schoenes, Phys. Reports **63**, 301 (1980).
- [17] S. Y. Savrasov, K. Haule, and G. Kotliar, Phys. Rev. Lett. **96**, 036404 (2006).
- [18] T. Miyake and F. Aryasetiawan, Phys. Rev. B, in press (2008), cond-mat 0710.4013.
- [19] S. Y. Savrasov, G. Kotliar, Phys. Rev. Lett. **90**, 056401 (2003).
- [20] X. Dai, S. Y. Savrasov, G. Kotliar, A. Migliori, H. Ledbetter, E. Abrahams, Science **300**, 953 (2003).
- [21] J. Wong, M. Krisch, D. L. Farber, F. Occelli, A. J. Schwartz, T.-C. Chiang, M. Wall, C. Boro, R. Xu, Science **301**, 1078 (2003).
- [22] P. G. Klemens, Phys. Rev. **148**, 845 (1966).
- [23] R. Brandt, G. Haufler, and G. Neuer, J. Non-Equilib. Thermodyn. **1**, 3 (1967).